Using Simulation for the Improvement of Manufacturing Operations in Medical Devices

Guido M. Quesada

Mechanical Problem Solving, S.A., San José, Costa Rica

Efraín Fernández

Boston Scientific de Costa Rica, S.R.L., El Coyol, Costa Rica

Abstract*: The solution of manufacturing problems in minimally invasive medical devices poses the quadruple challenge of a) providing solutions as soon as possible in order to maximize operation of the process lines, b) limiting the project to a budget which is considerably lower than usually allocated for R&D, c) obtaining results for fairly complex nonlinear problems with enough accuracy to detect the effect of dimensional variability in very small parts, and d) documenting the procedures thoroughly and formally for ulterior validation, approval and insertion into the product lifecycle management of devices whose impact on human lives is critical. This paper shows several cases in which these challenges are faced with the aid of nonlinear simulation using Abaqus/Standard. The assemblies include biopsy forceps with millimetric jaws driven by microwires, clamping systems for nested core wires and tubes, and crimped joints for rotatable retrieval devices. The models involve contact with large displacements and friction, relative play among the parts with significant sensitivity to dimensional variations, large plastic deformation and approved design constraints which limit significantly the range of possible modifications. The pressure of generating creative and effective solutions opportunely and presenting results in a formal and convincing way elevate the degree of difficulty. This calls for models that can be modified parametrically within the simulation environment and run very quickly. Abaqus/Standard provided excellent resources such as surface/surface contact, soft contact, cuasi-static modeling as dynamic-implicit, in order to tame models which are in most cases intrinsically unstable.*

Keywords*: Assembly Deformation, Bending, Design Optimization, Elasticity, Experimental Verification, Forming, Hyperelasticity, Interface Friction, Mechanisms, Medical Devices, Plasticity, Residual Stress.*

1. Introduction

The medical device industry sector in Costa Rica has grown 283% during the last ten years, faster than any other manufacturing sector, to become one of the main export activities and sources of foreign investment. Two examples of medical devices, which are manufactured by Boston Scientific, are biopsy forceps and polyp removal devices.

A biopsy forceps is a disposable forceps used during minimally invasive gastro-intestinal and urologic endoscopy for collecting biopsies. A typical biopsy forceps has a pair of jaws on one end of a catheter (typically a coated or sheathed steel coil) which is inserted in the body and an operating handle on the opposite end. The jaws are opened and closed by means of a pair of microwires which travel inside the coil and are connected to the handle.

A polyp removal device is a disposable medical device used for the electrosurgical removal and cauterization of gastrointestinal tract polyps through an endoscope. The polyp is laced with a microwire rope loop. During insertion of the device into the body, the loop is collapsed inside a catheter. Once near final position the loop is pushed out of the catheter so it expands around the polyp. Then the loop is rotated with an actuator near the handle and finally pulled back thus cutting the polyp off and removing it from the body.

This paper shows recent examples of FEA simulations which have been used to address issues of product lifecycle which are discovered at the manufacturing stage. Because of the fast paced environment of the production lines, these problems must be resolved as quickly as possible, often after the R&D budget has been closed and still with high standards for the documentation and technical justification of every procedure.

2. Microwire mechanism for a biopsy forceps

A key requirement of biopsy forceps is a smooth and monotonic relationship between applied force and displacement at the handle with respect to the resulting opening or closing motion of the jaws on the distal end of the device and the biting force they apply on the tissue. If the surgeon feels irregular response or clicking, it may be a sign that the device is not performing correctly.

As found by experiments and by FEA simulation, monotonic and smooth handling is strongly related to the shape of the microwires as they exit the coil and engage with the jaws. Subtle changes in the jaw’s arm length as well as the curve of the wire ends can make a significant difference.

2.1 FEA model

The model used includes two jaws and a coil which are represented as rigid surfaces. Another rigid part (not shown) is a clevis which holds the coil and the jaw axle together. The coil is fixed, while the jaws are allowed to rotate about a fixed axis. The wires, as well as the needle, are modeled as deformable bodies with a fairly fine mesh. Although several parts in the assembly are identical, their position is not necessarily symmetric. Therefore no planes of symmetry can be used. It is important to capture the interaction between the wires and the jaw eyelets, the needle and the coil.

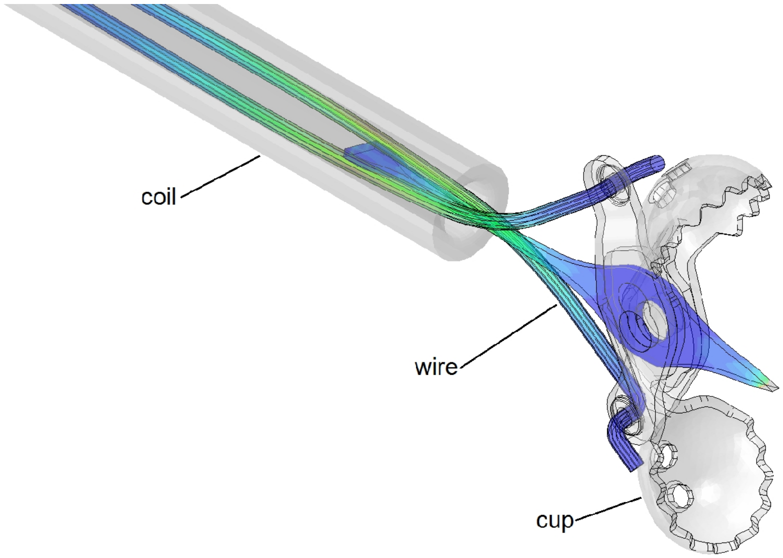

Figure 1. Biopsy forceps model

A main aspect of interest in the system's structural behavior is how the microwires, which are initially curved, straighten or bend further as the jaws move towards the open or closed position, and how this affects the reaction that is perceived by the operator at the handle. Another aspect is the interaction of the wires with the inner surface of the coil. Relatively high contact forces and displacement around the edges were identified as a possible cause of clicking or scraping. It was found that this interaction changes considerably as the jaws open or close.

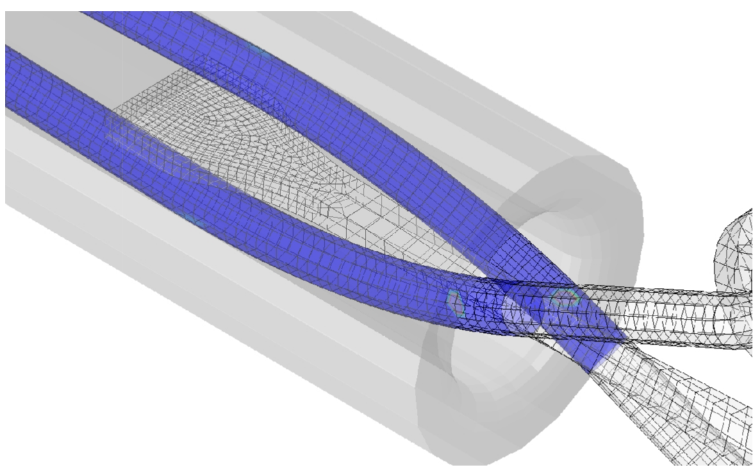

Figure 2. Detail of wire-coil interaction

Adequate calibration of soft contact between the parts enabled smooth and stable model behavior. Hard contact would expose the irregularities in sliding due to the mesh discretization, while excessively soft contact would produce variations which are beyond the dimensional tolerances. Exponential soft contact proved effective, using a distance of 0.0002” for zero contact pressure and a pressure similar to the yield stress of stainless steel at zero distance.

2.2 Dimensional scenarios

Dimensional scenarios involve variations in the jaw’s arm length and location of the rotation axis, as well as the wire curve radius, length and angle. Both FEA and experimental exploration confirmed that subtle changes in these parameters would produce changes in the device’s behavior which could be felt at the handle. However, the relationship between these parameters and the resulting changes were unclear. This made it difficult to determine which adjustments in wire curve would be necessary in order to achieve optimal performance.

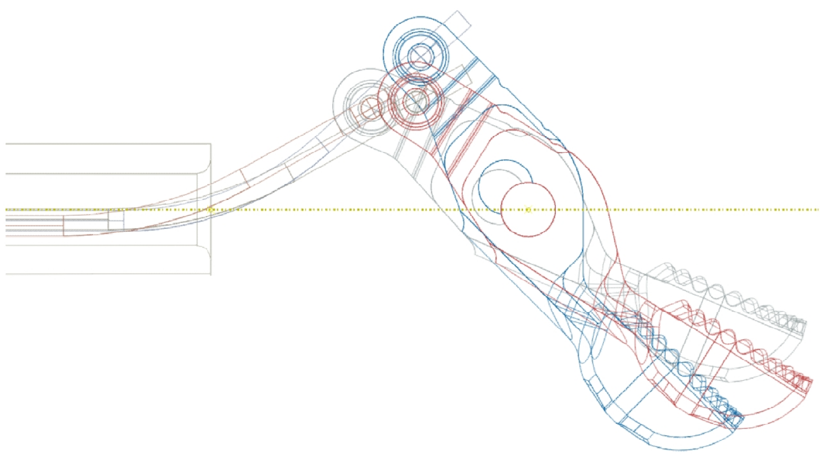

Figure 3. Sample dimensional scenarios of jaws and microwires

2.3 Characterizing jaw-wire interaction

Although it doesn’t appear intuitive, a plot of reaction moment at the jaw’s rotational axis vs. jaw rotation angle proved to be the most useful in order to characterize the system’s behavior in the most general way. At some point between the open and closed position, there is a reversal in the reaction moment. This reversal is a key aspect of the characterization, since it can be associated with a snap-through between open and closed position, as the microwires are pulled (closing or biting action) or pushed (opening action) by the surgeon.

Furthermore, the working environment and resulting tension in the microwires can vary. In some instances the surgeon may be just exercising the device or trying to capture a thin piece of tissue, so tension is relatively low, whereas in other instances it may be necessary to bite a piece off, which requires greater tension. In all circumstances, the surgeon must be able to feel a smooth and monotonic response to the operation of the handle. Therefore the analysis should be independent of wire tension.

Snap-through is also a source of numerical instability in a cuasi-static analysis, while a dynamic analysis might introduce inertial effects which obscure the measurement of relatively small forces. By prescribing a rotational angle at the jaw, instead of applying tension or displacement of the wires (which would appear more intuitive), wire tension was taken out of the picture. Also in this way a cuasi-static model became more stable and enabled the exploration of the system at every position of the jaws.

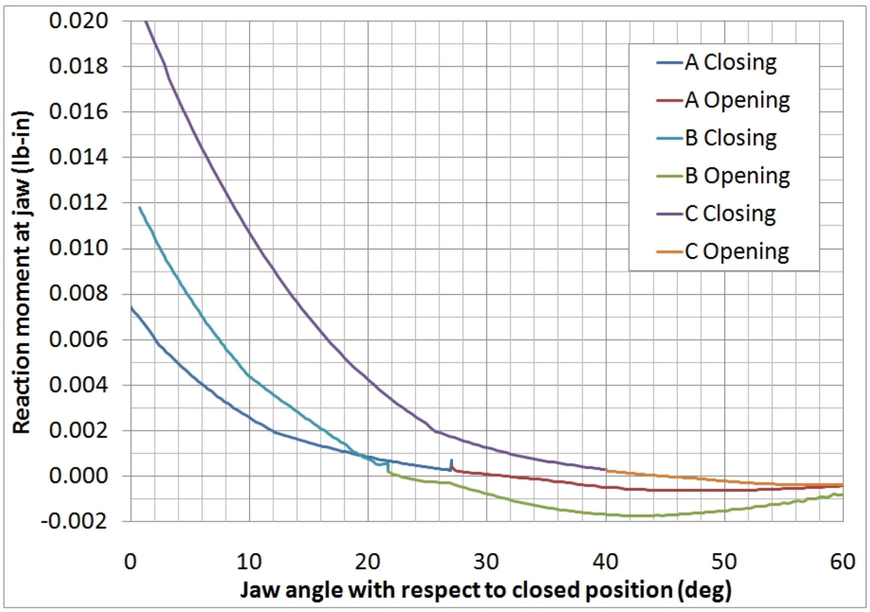

Figure 4. Relationship between jaw rotation and reaction moment

2.4 Results and experimental verification

The simulation was able to identify a range of wire curve design parameters which would produce optimal operation. Once the FEA lead to a promising range of parameters, the results were further explored and validated by extensive physical testing. Although the FEA did not produce explicit expressions that would enable direct calculations of adequate part dimensions, it did provide the tools to observe their potential behavior and iterate towards optimal dimensions much faster and more economically than by experimental trial and error. It also provided a useful description and explanation of the interactions that occur in the system and how they can be felt by the operator.

3. Set screw insert assembly

One way of attaching microwires in a biopsy forceps to the actuator on the handle is to protect the wire (in this case called core wire) inside a stainless steel tube and fix them to a metal insert which is part of the handle assembly. The core wire and the tube are fixed using a set screw. In this application it is desirable to achieve the maximum pulling force while minimizing damage to tube and core wire. This must be done with a geometry as simple as possible, which can be machined easily and consistently on the metal insert.

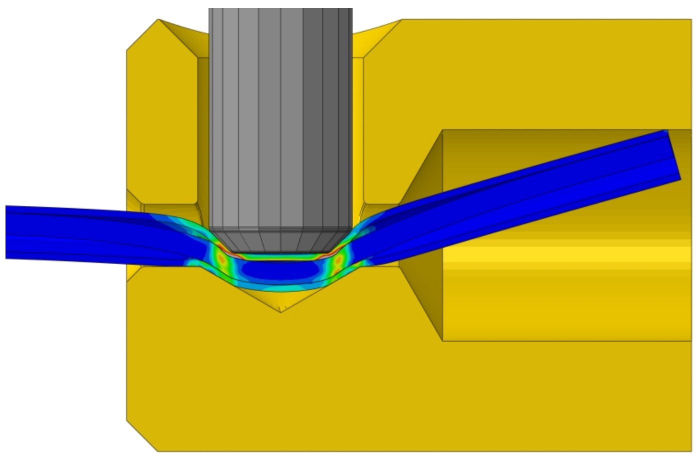

Figure 5. Plastic strain of core wire and tube fixed to the insert with a set screw

3.1 FEA model and dimensional scenarios

A fairly simple 3D model with one plane of symmetry was sufficient for this analysis. The insert and the tightening screw were modeled as rigid surfaces. The stainless steel core wire and tube were modeled as deformable bodies with elastic-plastic material properties.

An important simplification was the removal of the threads on the screw and the insert. Also for simplicity the tightening screw was pushed down without turning it at the same time. In fact the assembly has enough clearance to allow some misalignment. Therefore the model would not have a plane of symmetry. However in this case the priority was to obtain practical results as quickly as possible. Observation of sample assemblies led to the conclusion that lack of symmetry and the effect of turning the screw could be neglected. The simulation proceeds in two main steps. First the set screw is tightened up to a given torque (converted to resulting force for modeling purposes), then the core wire is pulled.

Several proposed configurations which were feasible from the manufacturing point of view were simulated in nominal dimensions. The scenarios involved changes in diameter, depth and bottom angle of the bores in combinations that would minimize the number of drill operations.

3.2 Characterizing tightening and pulling behavior

A torque vs. set screw displacement plot shows when adequate tightening is achieved. An initially steep curve becomes relatively flat as the tubing yields. Once the tubing is flattened around the core wire the curve becomes increasingly steeper as the tubing and the core wire are first bent and then compressed against the bottom of the step screw bore. Improved designs show a smooth behavior, which typically reflects a reduction in shearing of the tubing and the core wire.

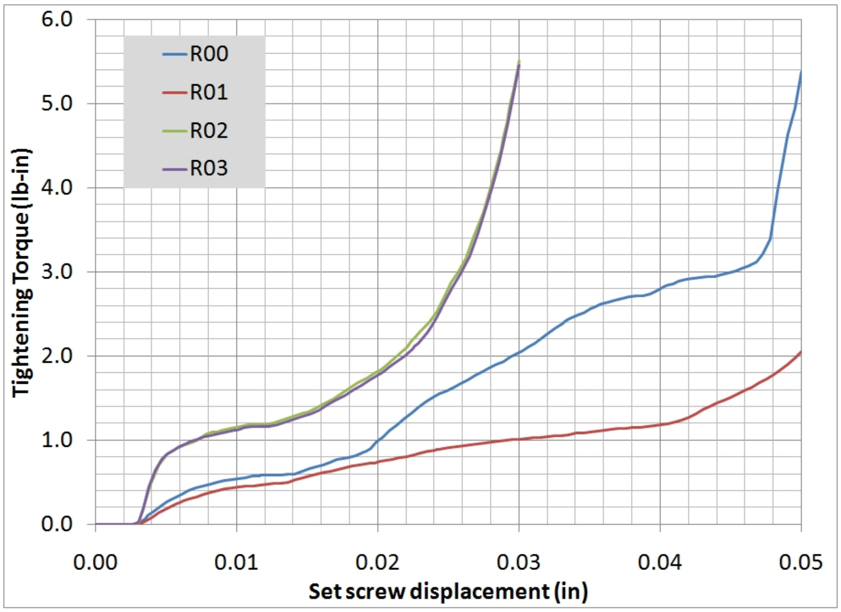

Figure 6. Set screw torque vs. displacement

Another important result is the pullout force. The best designs develop enough deformation to interlock the parts while accumulating less plastic deformation (as an indicator of material damage) on the tube and the core wire. As a result, the curve is steeper and the maximum pulling load is higher.

4. Crimped tubing around a wire coil

In a typical configuration the microwire rope loop is attached by means of a crimped piece of tubing to a set of three wires which transmit the pulling, pushing or rotating action coming from the handle. This joint must be able to pass standard pulling loads in order to make sure it will not come apart during operation. The tubing must be as small as possible in order to fit inside the catheter. Therefore optimization of the crimping process is critical.

4.1 FEA model and dimensional scenarios

Three pieces of wire coiled together and a piece of tubing covering the coil are made of stainless steel and modeled as deformable bodies with elastic-plastic properties. Three indenters placed around the assembly are modeled as rigid surfaces.

In a first step the indenters are pushed against the tubing to a prescribed position. Then they are removed. In a third step the wires are pulled out of the tubing and the pulling force is measured.

The mesh must be fine enough to capture the contact interaction between the wires and the indentation of the crimped tube by the indenters on the outside and the wires on the inside.

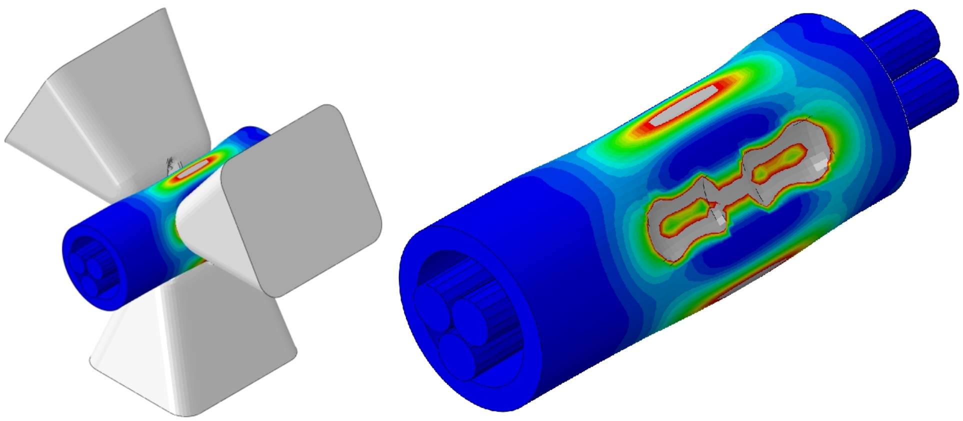

Figure 7. Wire and tube assembly during and after crimping

Multiple scenarios were studied in consideration of dimensional variation of the tubing, the wire coil and feasible adjustment of the indentation depth. Once critical scenarios were identified, several variations in indenter design were compared in order to determine which one would produce the strongest condition in terms of pullout force and minimal material damage.

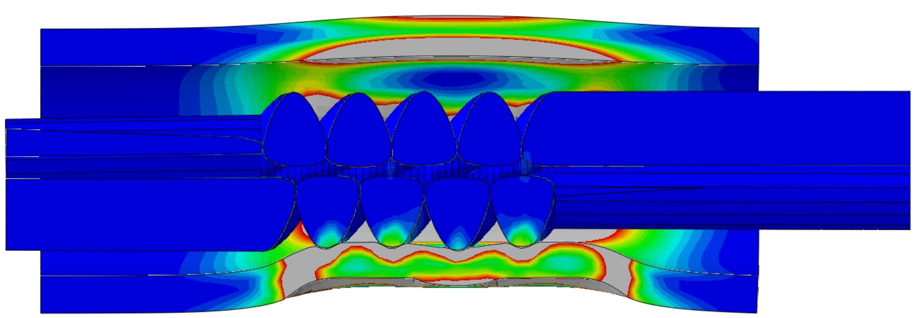

Figure 8. Cut view of the wire coil inside the crimped tube.

4.2 Results

The model was able to show and explain the mechanisms to improve reliability of the assembly in extreme dimensional scenarios, which were reproduced experimentally. The crimping must be deep enough to grip the wire coil but it should not be so deep that it would damage the tubing. An optimal indenter profile should be able to produce results which would be more tolerant to dimensional variations while avoiding excessive damage on the tubing. The analysis also established guidelines for the minimal tube wall thickness that can be used safely. Pull-out force vs. displacement force show the irregularity of the curves once the coils slide out of their grooves on the inside of the crimped tubing.

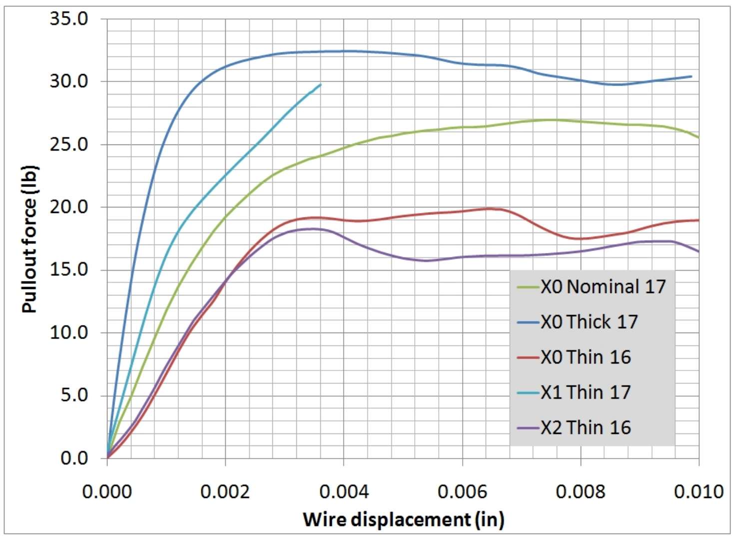

Figure 9. Wire and tube assembly during and after crimping

5. Microwire rope loop forming

The microwire rope which is used in polyp removal must be bent at several points in order to give it the desired shape. The loop must be able to collapse and fit inside catheter, and it must also be able to recover its shape when it comes out to capture the polyp. The manufacturing process by which these bends are formed determines how consistently the desired dimensions will be achieved and how able the loop will be to recover its shape.

In the present case a microwire rope is made of 7 strands with 7 wires each. The wires are less than 0.002" in diameter and the rope is about 5" long. This makes it virtually impossible to model the wire rope with finite elements in full detail (Erdonmez, 2009). Instead the first attempt is to represent the rope with an equivalent continuum model, which will exhibit the same bending and tension stiffness, as well as the same diameter in order to model contact with the forming tools.

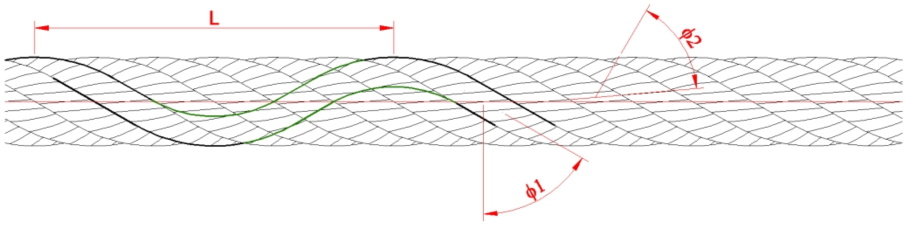

Figure 10. Typical wire rope

Nonlinear behavior of wire rope is fairly complex (Velinsky, 1985). Linear bending stiffness of a wire rope can be estimated according to the following equations (Gerges, 2008):

$$k_{cs} = \frac{E\pi D_w^4}{64}\left[1 + \frac{6\sin(\varphi_2)}{1 + \frac{\nu}{2}\cos^2(\varphi_2)}\right],$$

$$k_{gs} = \frac{E\pi D_w^4}{64}\left[1 + \frac{6\sin(\varphi_2)}{1 + \frac{\nu}{2}\cos^2(\varphi_2)}\right] \times \left[\frac{\sin(\varphi_1)}{1 + \frac{\nu}{2}\cos^2(\varphi_1)}\right] \text{ and}$$

$$k_{rope} = k_{cs} + 6k_{gs},$$

Where k_{cs} is the stiffness of the core strand, $k_{gs}$is the stiffness of a general strand, k_{rope} is the stiffness of all 7 strands combined, $D_w$is the individual wire diameter, $\varphi_1$is the helix angle of the strands and $\varphi_1$is the helix angle of the wires with respect to their strand.

The equations above can be used to estimate an elastic modulus for a continuum wire with equivalent bending stiffness. However, this underestimates axial tension stiffness. Similar equations were used to estimate axial tension stiffness. Then they were combined into a dual material model with a relatively soft body to provide most of the bending stiffness and a more rigid core for additional axial tension stiffness. The resulting elastic moduli were estimated with a simplified version of the combined equations as follows:

$$E_1 = 49E\frac{I_2A_w - A_2I_w}{I_2A_1 - A_2I_1},$$

$$E_2 = 49E\frac{I_1A_w - A_1I_w}{I_1A_2 - A_1I_2}$$

where E_1 is the core modulus, $E_2$is the body modulus, E is the modulus of the actual material, $I_1$and $I_2$are the corresponding moduli of inertia, $A_1$and $A_2$are the corresponding cross-section areas, I_w and A_w are the modulus of inertia and the cross-section area of a single wire. Equivalent yield stresses were also estimated, in order to model the forming of bends, by defining the strain at a bending radius that would produce yield in a single wire. It was assumed that tension loading alone will not produce yield stress. A model using embedded bar elements instead of a solid core was attempted, but it was numerically unstable. Although this approach appears more straightforward, it was discarded due to lack of initial results and time constraints.

5.1 FEA model

The only deformable body in this model is the wire rope. All other parts are rigid surfaces. These are a base head, a nose head, a nose hook and a pair of forming spools. In a couple of preliminary steps the wire is bent into a loop and the ends are inserted in the base head, then the middle of the wire is pulled by the nose hook and the first bend is made as the middle of the loop is folded inside the nose head. On the next steps the forming spools first make a couple of bends around the outside of the nose head then do the same around the base head. All these steps worked well as cuasi-static. Finally, the loop is released using an implicit dynamic step with cuasi-static damping settings, in order to obtain the final shape.

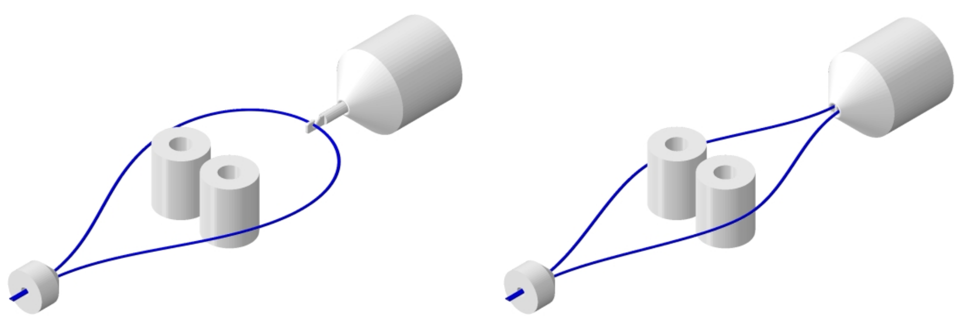

Figure 11. Wire rope before and after pulling the nose hook into the nose head

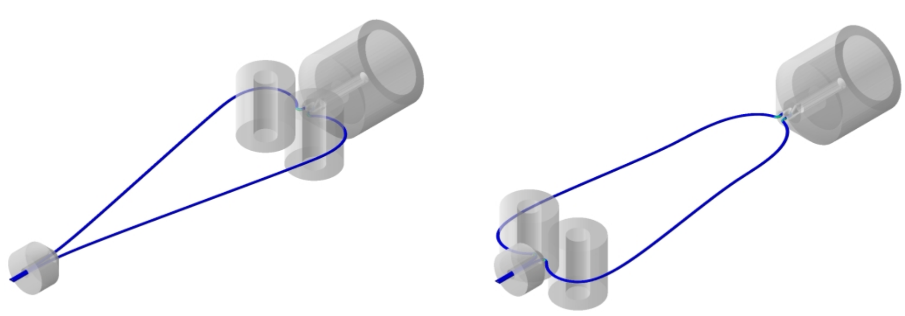

Figure 12. Wire rope loop during forming of the nose bends and base bends

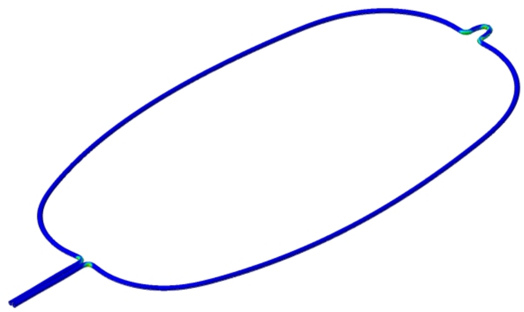

Figure 13. Wire rope after releasing it from the forming assembly

5.2 Results

This model is still under development. The first results are able to produce the loop width specified by design and detect dimensional variations that will occur with changes in forming load settings. However, the angles at the bends are closer than expected. This is most likely due to inaccurate calibration of the equivalent yield parameters in the FEA model. Further input data and experimental results are being collected in order to perform final adjustments.

Nevertheless, the study already provided useful insights as to how to dimension the forming heads and loops for each type of wire rope, in order to spread plastic deformation as much as possible, minimize superficial damage on the wire ropes and achieve bend radii which will be able to recover most of the intended shape after pushing the loop out of the catheter.

6. Rotational interaction between a square shaft and key

The wires which drive the loop in a rotational snare are turned with an actuator near the handle. This mechanism involves a rotational interaction between a hollow square shaft and a square key. The manufacturing process in such small dimensions requires dimensional tolerances which can leave a significant gap between the shaft and the key. Extreme dimensional scenarios can allow a tendency of the key to get stuck in the shaft. The mechanism is simple enough to allow algebraic calculation of the critical friction coefficient μ_{CR}, which is the friction coefficient at which the assembly would exhibit this tendency:

$$\mu_{CR} = \frac{\sqrt{(K_{CD} - 2K_{FR})^2 - (S_{ID} - 2K_{FR})^2}}{S_{ID}},$$

Where K_{CD} is the key circumscribing diameter, K_{FR} is the key fillet radius and S_{ID} is the shaft internal dimension.

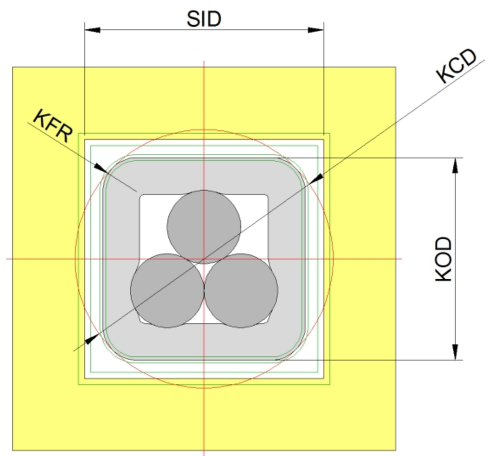

Figure 14. Basic key and shaft dimensions

6.1 FEA model and dimensional scenarios

A simple 2D plane stress model was used, with one deformable body for the hollow square shaft and one for the key (including the wires crimped inside the key). In a first step a reference pair of opposing forces was applied to the key in order to push it against the shaft walls. A very high friction coefficient is specified in order to make sure the parts would get stuck. This friction coefficient was defined as temperature dependant, so that by changing the temperature the friction will be reduced until the tangential interaction between the parts is overcome by normal reaction and the parts detach. This is identified as the critical coefficient defined earlier. The model was run for multiple combinations of shaft and key dimensions as allowed by dimensional tolerance.

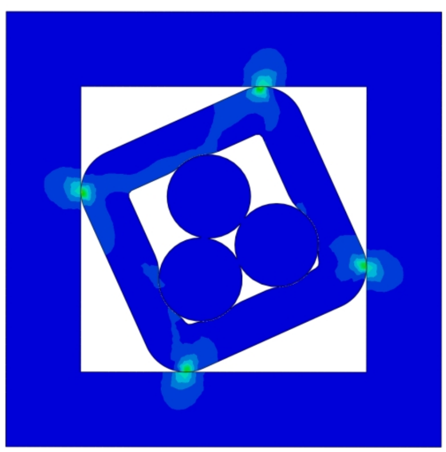

Figure 15. Stress pattern in shaft-key interaction

6.2 Results

FEA results show very small differences with respect to algebraic calculations in terms of critical friction coefficient. The differences can be attributed mainly to small deformations which are not taken into account by geometric calculations. This provided a good validation of the model and enabled to work with incomplete input data. Using these results it was possible to create a plot which allows the engineers to quickly identify the dimensional scenarios and lubrication conditions that should be avoided in order to guarantee optimal performance. This in turn was used to revise the dimensional specifications of keys and shafts.

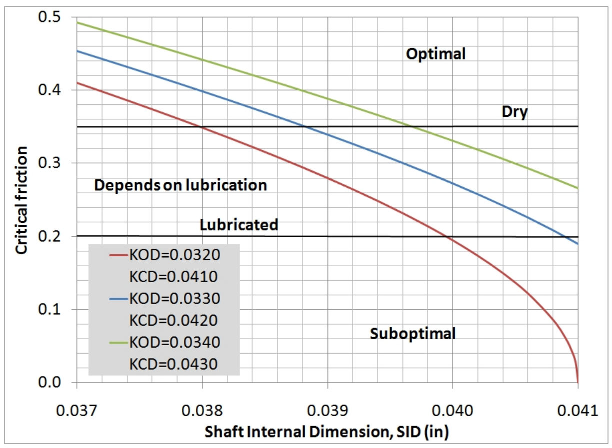

Figure 16. Critical friction vs. shaft ID for various combinations of key dimensions

7. Conclusions

The growing and increasingly sophisticated environment of the medical device manufacturing industry in Costa Rica provides an excellent ground to take advantage of high end mechanical simulation software such as Abaqus. All cases evaluated involve contact with friction, large displacements, gaps between parts in the assembly, with significant sensitivity to dimensional variations, plastic deformation, design constraints which limit significantly the range of possible modifications and protocols which demand extensive and convincing technical justification of every change to the process or the design.

Under these circumstances, fast, accurate and well presented results that can be obtained in the Abaqus/CAE system, on modest computer resources and under extreme time pressure typical of a manufacturing environment are decisive factors. The levels of confidence and technical complexity of these results are also opening the possibility for the research and development departments of companies such as Boston Scientific to take advantage of valuable information for design purposes, which is now being generated also at the manufacturing stage.

8. References

1. Gerges, Rafik R., “Model for the Force-Displacement Relationship of Wire Rope Springs,” Journal of Aerospace Engineering, ASCE, U.S.A., 2008.
2. Velinsky, S. A., “General Nonlinear Theory for Complex Wire Rope,” Int. J. Mech. Sci,Vol 27, No. 7/8, Great Britain, 1985.
3. Erdönmez, Cengiz and Imrak, C. Erdem, “Modeling and Numerical Analysis of the Wire Strand,” Journal of Naval Science and Engineering, Vol. 5, No. 1, 2009